NUMERICAL SIMULATIONS OF TURBULENT MIXING FACTOR IN 2×2 ROD BUNDLES AT SUPERCRITICAL PRESSURES

Jinguang Zang , Xiao Yan, Daiquan Du, Xiaokang Zeng, Yanping Huang
CNNC Key Laboratory on Nuclear Reactor Thermal Hydraulics Technology, Nuclear Power Institute of China

Abstract: Because of the importance of the turbulent mixing factor in changing the thermal hydraulics characteristics of rod bundles, the turbulent mixing phenomena was investigated based on the CFD numerical simulation in 2×2 rod assembly at supercritical pressures. The various energy transport effects were analyzed including both the diversion cross flow and turbulent fluctuation of nature mixing. A new method based on the energy mixing concept was proposed and compared with other methods. It was found that the energy turbulent mixing was largely dominated by the local enthalpy gradient which could differ from the average enthalpy difference between two adjacent subchannels. So there could be possibility of existing negative turbulent mixing factor under some occasions. Finally, the comparison of CFD results with subchannel code was made which could provide a proof of the reasonability of this method.
Keywords: turbulent mixing, CFD, subchannel,

1. Introduction

Supercritical Water Reactor (SCWR) has been selected as one of the generation IV power conversion systems due to its high thermal efficiency, compact system design and technology incorporation from both the supercritical fossil plants and regular pressurized water reactors. The preliminary design work has been performed in many countries (OKa et al. 2010; Schulenberg et al. 2010; Torgerson et al. 2006). Plenty of research activities focusing on the SCWR background are under way including basic heat and flow mechanism, flow instability, heat transfer deterioration, critical flow, fuel assembly design and so on (Pioro 2007).

The thermal hydraulic behavior in fuel assembly is very important for the design work to ensure the core’s safety and economy. But due to the rigorous limit imposed by the high pressure and high temperature condition, very few experiments were performed and hardly provided enough information about what was going on in the rod subchannels. Dyadyakin and Popov (1977) performed experiments of 7-rod tight lattice bundles under the pressure of 24.5 MPa, mass flux 500-4000 kg m^{-2} s^{-1} and heat flux less than 4.7 MW m^{-2}. The pressure oscillation was observed during the experiments when the heat flux was increased to some extent. Richards et al. (2011) used R-12 as the coolant to investigate the heat transfer characteristics in 7-rod bundle. Razumovskiy et al. (2008) and Razumovskiy et al. (2009) performed experiments in vertical annuli, 3-rod, 7-rod bundle with supercritical water and the heat transfer deterioration was observed. Misawa et al. (2009) performed 7-rod bundle experiments and thought that the grid spacer could enhance the heat transfer ability. Besides the experimental study, many researchers studied supercritical flow by CFD methods (Gu et al. 2008; Gu et al. 2010; Yang et al. 2007; Shang 2009; Zhu and Laurien 2010). It is generally acknowledged that there is non-uniform distribution of flow field and temperature field in the rod bundles, especially the wall temperature at the fuel rod wall.

Most previous research about rod bundles has been focused on the heat transfer characteristics, the wall temperature distribution, and the secondary flow pattern and so on, but seldom refers to the turbulent mixing phenomena in such complex geometry and fluid property variation. Gu et al. (2008) performed pioneer work in proposing a calculation procedure based on the CFD results and some interesting phenomena was noticed. Further investigations are still needed.

In subcritical conditions, various experimental techniques have been used to study mixing in rod bundles such as the use of the direct subchannel enthalpy measurement, hot water injection, wire-mesh sensor technique and chemical or radioactive tracers (Sadatomi et al. 2004; Silin et al. 2004; Hwang et al. 2000). The common procedure is to measure either subchannel temperature or tracer concentration and then attempt to predict the experimental measurements with a subchannel code by adjusting coefficients in an assumed mixing correlation. These procedures could provide good reference for related research of supercritical water.

In this paper, the turbulent mixing phenomena were investigated based on the CFD techniques in 2×2 rod bundles under supercritical conditions. A new method of calculating turbulent mixing factor was proposed up and a strange phenomenon of negative turbulent mixing factor was observed. The reason behind this was discussed.

2. Computational Procedures

2.1 The geometry parameter of 2×2 rod bundle

In the present study, the 2×2 rod bundle is considered as the calculation object, indicated in Fig. 1. Due to geometry symmetry, only one-eighth of the rod bundle is taken for the CFD analysis. The 2×2 rod bundle consists of three kinds subchannels which are very typical for thermal SCWR fuel assembly design : One center subchannel, four side subchannels and four corner subchannels, shown in Fig. 2. The center subchannel is surrounded by four pieces of fuel rod claddings and is located in the center of rod bundle. The side subchannel located at the brink is surrounded by two pieces of fuel rod claddings and a part of the fuel assembly box. The corner subchannel located at the corner of the rod bundle is encircled with one piece of fuel rod cladding and a box corner. The 2×2 rod bundle is considered to be the simplest channel type which consists of all these three typical subchannels. The fuel rod diameter is 9.5mm with the pitch of 10.5 mm. The gap between the fuel rod and the bundle box is 1 mm which is designed to decrease the side wall effect on the thermal hydraulic characteristics.

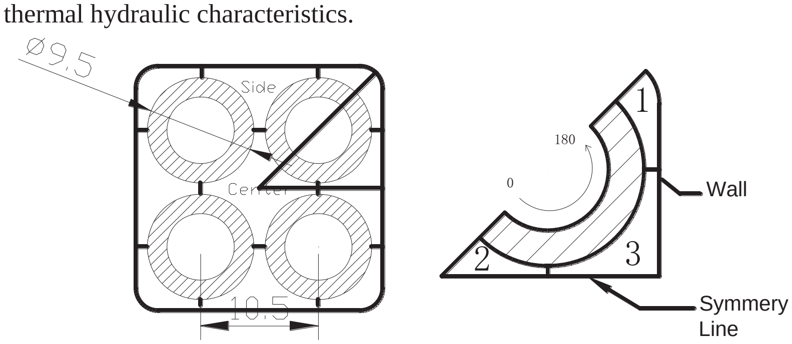

Fig. 1 Scheme diagram of 2×2 rod bundle

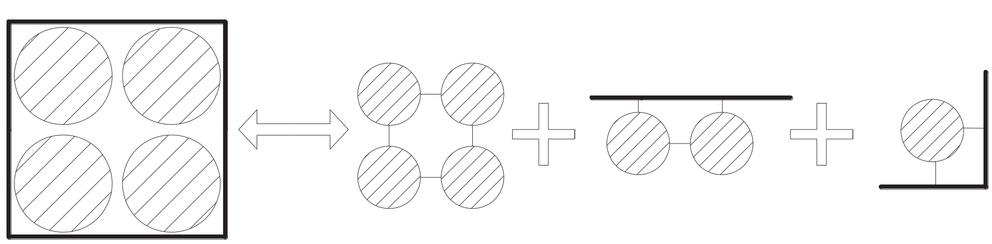

Fig. 2 Typical subchannel for 2×2 rod bundle

2.2 Selection of turbulence models

The selection of turbulence model is always a very puzzling question. The paradox is that the mechanism the turbulence model is based on and its behaviors in reality don't always agree well. The good performance of one turbulence model in one case doesn't promise in another case. This is the situation for turbulence model in supercritical water applications especially when trying to predict the starting point of heat transfer deterioration. It is acknowledged that the common turbulence models developed under subcritical conditions can't be directly and completely extrapolated to supercritical conditions when the fluctuation of fluid property is not negligible. However, in some cases when the heat transfer is not seriously affected by the strong non-equilibrium forces of buoyancy or acceleration, the common turbulence models seem to show a good agreement with the experiments. Lots of research work supports this, although an agreement is hardly to reach on which is the most suitable turbulence model.

Some researchers suggested SST (Shear Stress Transport) turbulence model was relatively better in predicting heat transfer deterioration problem (Palko and Anglart 2008, Huang et al. 2012, Wen and Gu 2011). The SST turbulence model was designed to effectively blend the robust and accurate formulation of the k-ω model in the near-wall region with the free-stream independence of the k-ε model in the far field. The major ways in which the SST model differs from the standard model are as follow:

Gradual change from the standard k-ω model in the inner region of the boundary layer to a high-Reynolds-number version of the k-ε model in the outer part of the boundary layer

Modified turbulent viscosity formulation to account for the transport effects of the principal turbulent shear stress

These two features make the SST k-ω model more accurate and reliable for a wider class of flows than the standard k-ω model. Other modifications include the addition of a cross-diffusion term in the ω equation and a bending function to ensure that the model equation behave appropriately in both the near-wall and far-field zones. Besides this, another important reason that makes the SST model so popular is its robust characteristics in dealing with complex geometry flows in industry applications. Other low Reynolds number models often fail to give reliable predictions in this aspect and limit their further applications.

The comparisons with the experiments performed in Nuclear Power Institute of China (NPIC) in vertical circular tube of 6-mm diameter with supercritical water confirmed its appropriateness as depicted in Fig. 3. The results show that SST turbulence model has the potential to capture the heat transfer deterioration phenomenon; though the prediction error starts to get increased as the operating pressure is closing to the critical point. In the present study, the SST turbulence model is selected.

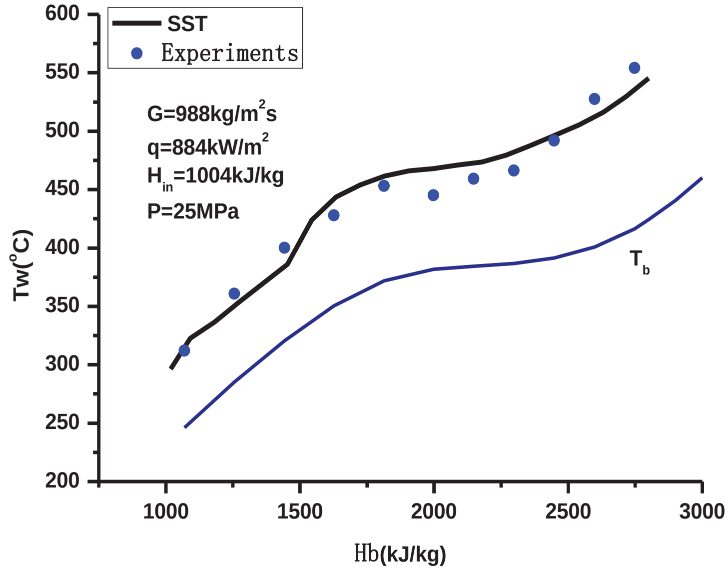

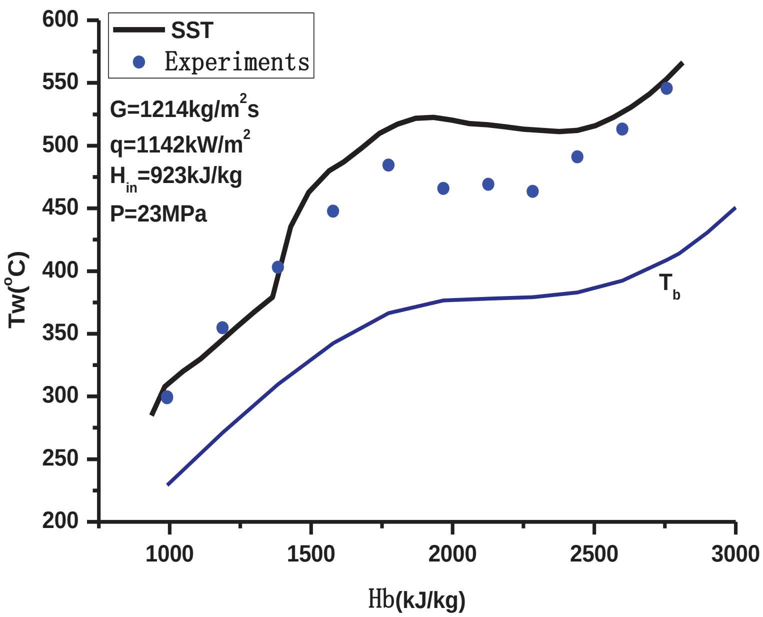

Fig. 3 Comparison of predictions with experimental data

2.3 Mesh sensitive test

The structural meshes are generated in order to carefully adjust the mesh parameters in the boundary layer. The possible solution dependence on mesh is examined with 4 different kinds of meshes shown in Fig. 4. The mesh parameter is listed in Table 1. The mesh sensitive test was checked by comparing the average local friction coefficient *f* and heat transfer coefficient *h* with the following definitions:

$$f = 4\frac{\overline{\tau}}{\frac{1}{2}\rho u^2}, \quad \overline{h} = \frac{q_w}{\overline{T_w} - T_b} \qquad (1)$$

Here, $\bar{\tau}$ is the length average of the wall shear stress circling around the rod at specified location; q_w is the wall heat flux imposed on the rod surface. ρ, u and T_b are fluid density, fluid velocity and fluid temperature averaged over the cross section, respectively. T_w is the length average of wall temperature.

The results show that when the node numbers are greater than or equal to 1,200,000, the solution doesn't depend on the mesh numbers. Finally, the No.3 mesh was chosen for conservation.

Table 1 Mesh Parameters

No.	Mesh Numbers
No.1	900,000
No.2	1,200,000
No.3	2,300,000
No.4	4,600,000

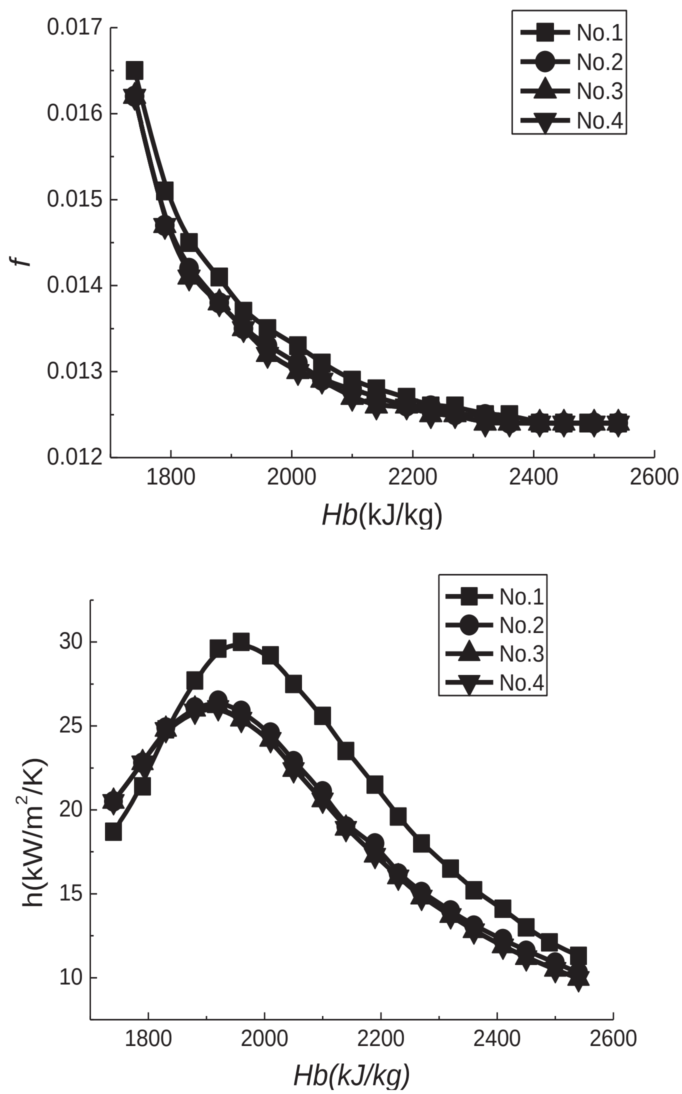

(a) (b)

Fig. 4 Mesh sensitive test (a) friction coefficient (b) Heat transfer coefficient

3. Results and discussions

3.1 The energy exchange at the interface

The energy variation for coolant in one subchannel depends on these principle factors: the heat imposed by the rod surface; the volume heat flux or volume force work, the energy exchange at the interface. The energy exchange at the interface between adjacent subchannels can be classified into two groups: the forced mixing and natural mixing. The forced mixing can be further decomposed of flow scattering and flow sweeping caused by support structures in the flow channels, e.g. grid spacers, ribs or mixing vanes. The natural mixing consists of diversion cross flow and turbulent mixing. The former is mainly driven by the transversal pressure gradient between adjacent subchannels, while the latter is most contributed by non-directional eddy motion across the gap. This process of eddy motion was found to be related to the phenomenon of quasi-periodic pulsations governed by the presence of coherent structures.

Considering a subchannel control volume, the energy conservation equation is:

$$Q_{in} + Q_{heat} + Q_{crossflow} + Q_{turb} = Q_{out} \qquad (2)$$

The Q_{in} stands for the inlet heat flux, Q_{out} outlet heat flux, Q_{heat} the heat imposed by the wall. $Q_{crossflow}$ and Q_{turb} represent the heat contributed by diversion cross flow and turbulent mixing, respectively. Their expressions are listed below:

$$Q_{in} = \int_{A_{in}} (\rho U H) dA \qquad (3)$$

$$Q_{out} = \int_{A_{out}} (\rho U H) dA \qquad (4)$$

$$Q_{heat} = \int_{S_{rod}} q dA \qquad (5)$$

$$Q_{crossflow} = \int_{A_{gap}} \rho V_{cross} H dA \qquad (6)$$

All the information necessary to calculate these four terms could be provided by the CFD simulation results. Then according to the energy conservation equation, the heat transport by turbulent mixing Q_{turb} is calculated with this:

$$Q_{turb} = Q_{out} - (Q_{in} + Q_{heat} + Q_{crossflow}) \qquad (7)$$

The 2×2 rod bundle consists of three kinds of subchannels: Center subchannel, corner subchannel and side subchannel and two kinds of interface types: the interface between center subchannel and side subchannel named interface *a* and the interface between the side interface and corner interface named interface *b*. Based on the aforementioned energy conservation method, we could obtain the turbulent heat flux at interface *a* from center subchannel equation, and that at interface b from corner subchannel equation. Ten sections were divided along streamwise directions, and then the turbulent heat mixing could be calculated at each section.

Fig. 5 illustrates the varied profile of heat contributed by diversion cross flow and the turbulent mixing at the interface *a* along the axial flow direction. Consider the center subchannel as the control volume. Define these two effects positive when they tend to add heat to the center subchannel and negative vice versa. From Fig. 5, the diversion heat cross flow is positive before axial position 0.7m and negative after that. The heat transported by the diversion cross flow is larger than that by turbulent mixing. The heat transported by crossflow is about 250W for each control volume at the inlet section and decreases till it maintains at the value of -50W, while the heat transported by turbulent mixing is the value of about 10W. Although the heat transported by crossflow is large at the absolute value, it contributes not that much with consideration to the mass flow transported synchronously. The heat transported by turbulent mixing stands for the net heat exchange without mass exchange which would contribute a lot to the average enthalpy of that subchannel. Fig. 6 gives the picture of the heat transported by the two effects at the interface b with the side subchannel as the considered control volume. The relative magnitudes of these two effects are similar as that at interface *a* except the positive or negative sign.

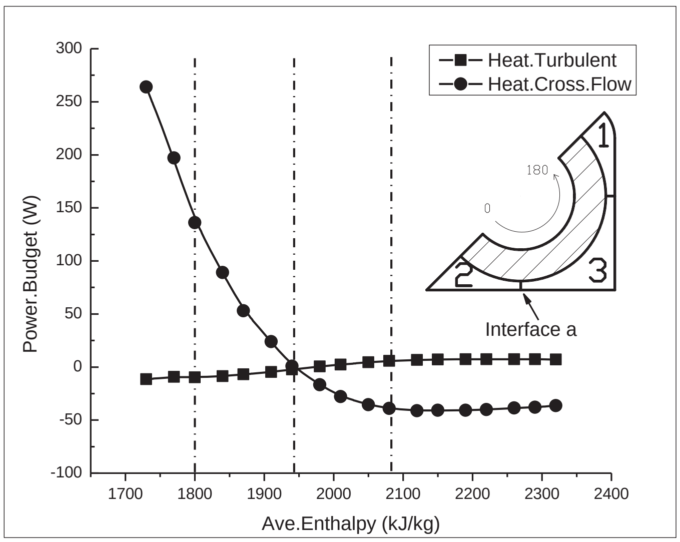

Fig. 5 The heat transported by diversion cross flow and the turbulent mixing at interface *a*

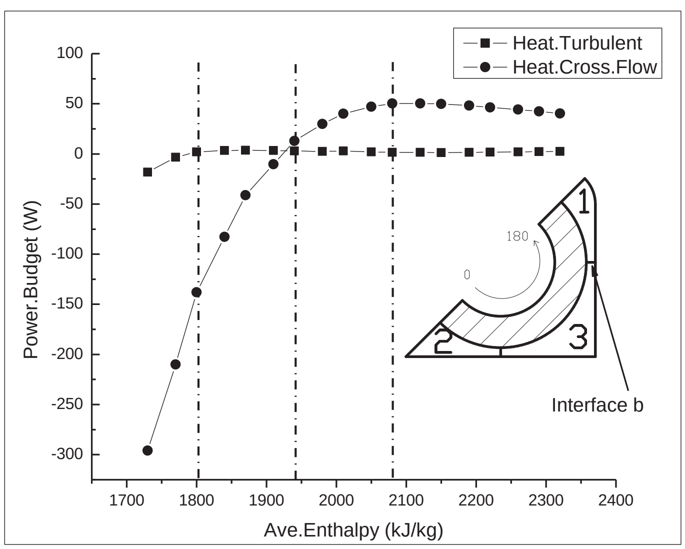

Fig. 6 The heat transported by diversion cross flow and the turbulent mixing at interface *b*

The different sign of positive or negative represents that the cross flow direction has been changed during the flow process which implies that the driven force behind the crossflow is also changed. It has been found that the mass flow redistribution is related to the secondary flow at the cross section driven by pressure gradient. At the upstream, the driven force mainly rises from the different flow resistance between adjacent subchannels. As the center subchannel has the biggest hydraulic diameter among these three kinds of subchannels, the flow resistance is relatively small. Then the fluid from other two subchannels tends to flow into it. So at the beginning, the driven force is mainly caused by flow resistance caused by geometry factor. At he downstream, when the fluid at the center subchannel gains heat and crosses the pseudocritical point, fluid volume will expand due to the quick decrease of the fluid density and push the fluid outward to other subchannels. So at the latter stage, the main influence factor is the fluid property variation in crossing the pseudocritical point. Fig. 7 presents the secondary flow patterns at different locations. When the location is at 0.3m, the secondary flow is clockwise; when at the location of 0.7m, the flow direction starts to reverse though the magnitude is very weak; then the counterclockwise secondary flow is getting bigger in the downstream.

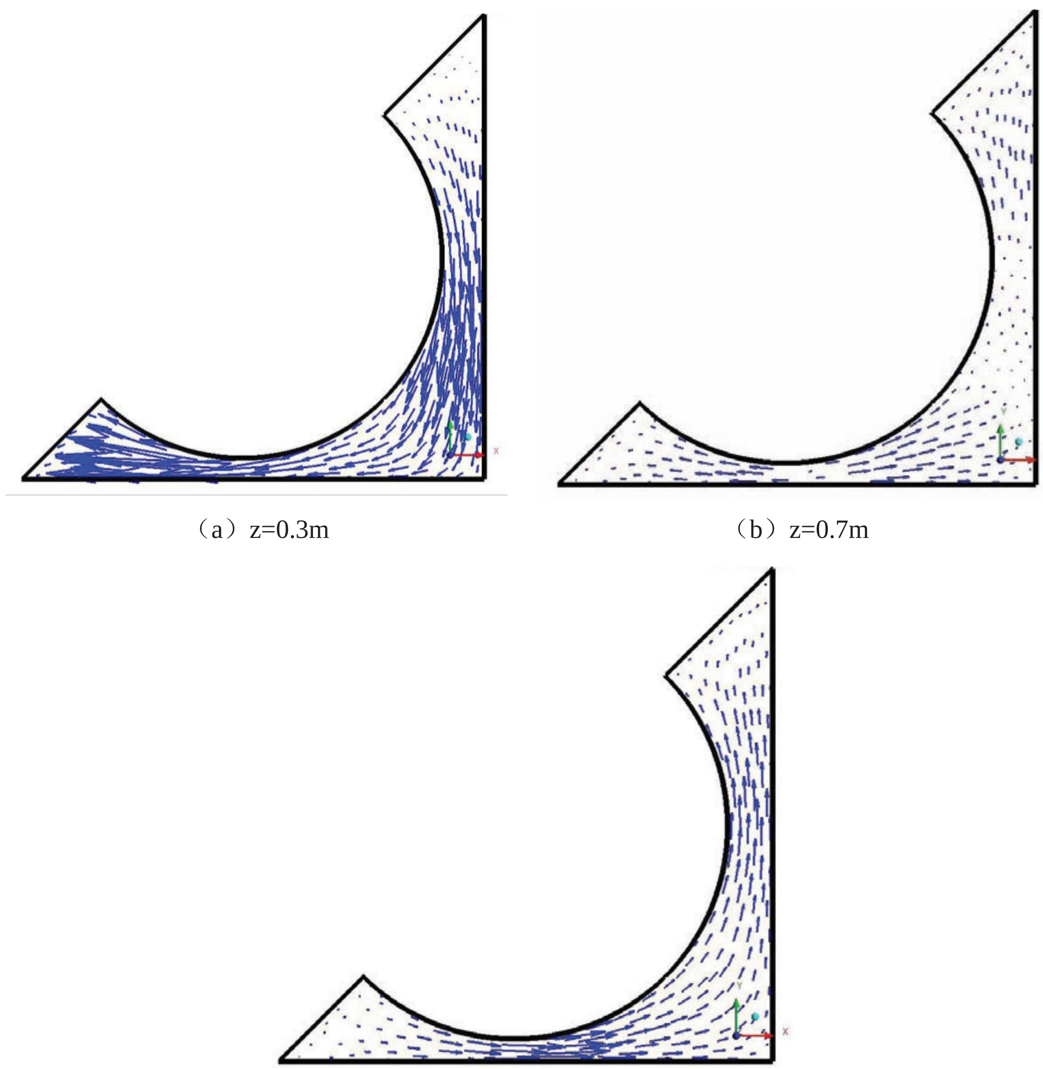

（a）z=0.3m

（b）z=0.7m

（c）z=1.1m

Fig. 7 Secondary flow at different locations

3.2 Turbulent mixing coefficient

The turbulent mixing plays an important role in enhancing the momentum and heat transfer between two adjacent channels. Here we propose a method of calculating the turbulent mixing coefficient based on the Computational Fluid Techniques. As we know, the turbulent mixing is related to the fluctuation eddy motion at the interface which is hard to get from a subchannel analysis code focusing on the average subchannel result. Computational Fluid Dynamics, however, could provide a more detailed picture of the turbulent field in the rod bundles so that it can be used to complement the shortcomings of subchannel analysis code. The basic idea is based on the equivalent heat contribution by both description scales that the time averaged turbulent motion in CFD calculations contribute the same as that calculated by subchannel analysis code with turbulent mixing factor in heat exchange in adjacent channels.

According to the definition of thermal turbulent mixing coefficient:

$$q_{ij} = -\overline{\rho u_i^{'} h^{'}} = \beta \Delta H_{ij} \overline{G_{ij}} \qquad (8)$$

In CFD simulations, the turbulent heat flux can be modeled with the multiplication of eddy viscosity and the gradient of enthalpy.

$$-\overline{\rho u_i^{'} h^{'}} = \frac{\mu_t}{\mathrm{Pr}_t} \frac{\partial h}{\partial x_i} \qquad (9)$$

Pr_t is the turbulent Prandtl number representing the similar factor between the turbulent momentum transport and heat transport. Pr_t is often selected to be 0.85 in most cases.

Combing equation (8) and equation (9), then we get the calculation expression of turbulent mixing coefficient:

$$\beta = \frac{\mu_t}{\mathrm{Pr}_t} \frac{\partial h}{\partial x_i} / \Delta H_{ij} / \overline{G_{ij}} \qquad (10)$$

All these quantities could be provided by CFD calculation results. ΔH_{ij} is the enthalpy difference of subchannel *i* and subchannel *j*. G_{ij} is the average mass flux of subchannel *i* and subchannel *j*.

As mentioned above, the turbulent mixing coefficient could also be calculated based on the energy balance method. As the energy balance is computed over a control volume, the turbulent mixing factor obtained by this way is the average value of the factor for the whole interface of the control volume. The averaged length scale is dependant on that of control volume. This method is limited to simple subchannel layout which hard to be applied to complex geometry where the number of established energy equations could be less than the unknown variables.

Gu et al. (2008) proposed another method of calculating turbulence mixing factor with CFD simulation results based on the assumption that the probability distribution of velocity fluctuation satisfies the Gauss distribution. The turbulent mixing factor is calculated in this way:

$$\beta = \frac{\sqrt{\overline{vv}}}{\sqrt{\pi} U} \qquad (11)$$

Here U is the axial average velocity in subchannels; $\overline{vv}$ is transverse Reynolds stress across the gap which could be directly obtained from CFD analysis calculated by Reynolds Stress kind turbulence model. While for the eddy viscosity model, with the isotropic turbulence behavior assumed, the transverse Reynolds stress is:

$$-\rho\overline{vv} = \mu_t \frac{2\partial v}{\partial y} - \frac{2}{3}\rho k \qquad (12)$$

And the turbulent mixing factor:

$$\beta = \sqrt{\frac{2}{3}k - \frac{\mu_t}{\rho} 2\frac{\partial v}{\partial y}} / \sqrt{\pi} / U \qquad (13)$$

This method means that the fluctuation velocity at the gap directly contributes to the net exchange of heat and momentum transport. In fact, turbulent eddy motion in CFD results only contributes to the exchange at the local scale and is related to the local enthalpy gradient. The turbulent mixing factor, however, is a measure of mixing phenomena at subchannel scales. Applying the local mixing factor to represent the average one may overestimate the actual mixing intensity.

Now we summarize the three methods of calculating turbulence mixing factors and make a comparison.

(1) The Energy Mixing Method

$$\beta = \frac{\mu_t}{\mathrm{Pr}_t}\frac{\partial H}{\partial x} / \overline{G} / \left(H_i - H_j\right) \qquad (14)$$

(2) The Energy Conservation Method

$$\beta = q_{ij} / \Delta H_{ij}\overline{G_{ij}} = \frac{Q_{Turb}}{A_{gap}\Delta H_{ij}\overline{G}_{ij}} \qquad (15)$$

(3) The Turbulent Motion Method

$$\beta = \sqrt{\frac{2}{3}k - \frac{\mu_t}{\rho} 2\frac{\partial v}{\partial y}} / \sqrt{\pi} / U \qquad (16)$$

Fig. 8 shows the comparison of turbulent mixing factors along the flow direction by those three methods at interface *a* and interface *b*. The turbulent motion method predicts the largest value among them with the magnitude of 0.035 and 0.05 at both interfaces, respectively. The energy conservation method and energy mixing method predict generally similar magnitudes especially at the downstream. This could prove the reasonability of the Energy Mixing Method to some extent.

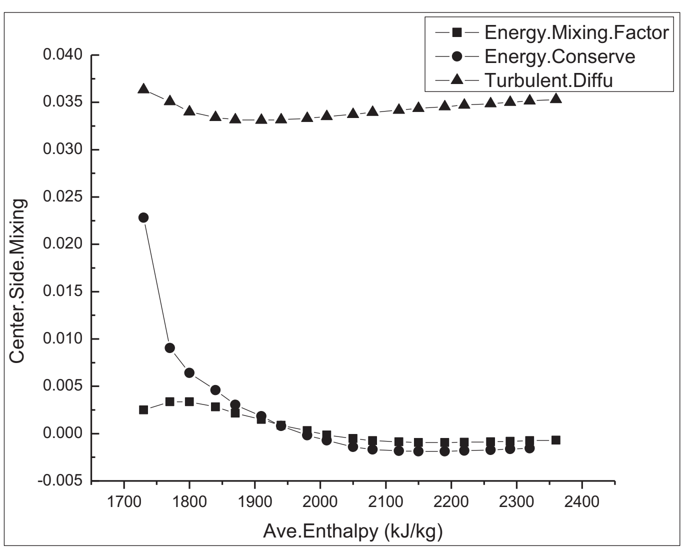

(a)interface a

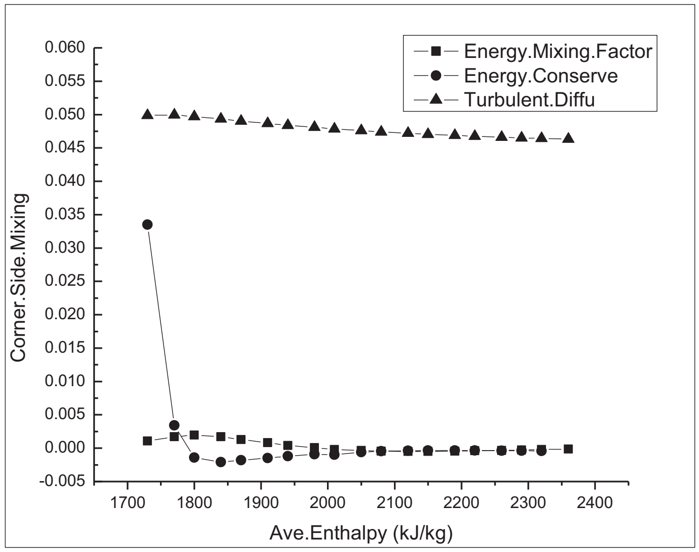

(b)interface b

Fig. 8 Comparison of three calculation methods

The turbulent mixing has always been considered to help decrease the enthalpy difference between adjacent subchannels. The high enthalpy fluid will make exchange with the low enthalpy fluid leading to the energy flowing from hot channel to cold channel, which would reduce the non-uniform distribution of fluid temperature thus enhance the safety of the rod bundles. But the enthalpy gradient is different in subchannel scale and local CFD scale. The average fluid temperature of hot channel is higher than that of cold channel which doesn't promise the same conclusion at the subchannel interface. The local enthalpy gradient at the subchannel interface may have the opposite sign with the average enthalpy gradient at the subchannel level. In this case, the energy will not flow from hot channel to cold channel, but in opposite direction which needs attentions because of the possibility of endangering reactor safety.

Fig. 9 presents the variation of turbulent mixing factor calculated by Energy Mixing Method along the flow direction at two interfaces. The turbulent mixing factors are both positive after the inlet and increase a little till they reach their peak. And then they start to decrease from positive to negative and change little after they get to the minimum value. From Fig. 8, the turbulent mixing factor calculated by Energy Conservation Method is also negative at the latter stage which may tell us that such phenomena may be reasonable.

According to the method proposed up in this paper:

$$\beta = \frac{\mu_t}{\Pr_t}\frac{\partial H}{\partial x}/\overline{G}/\left(H_i - H_j\right) \qquad (17)$$

When β<0, which means $\frac{\partial H}{\partial x}/\left(H_i - H_j\right) < 0$, the local enthalpy gradient at the interface $\partial H/\partial x$ is opposite with the enthalpy difference of subchannel i and j.

Fig. 10 shows that the average enthalpy of center subchannel is bigger than that of side subchannel which is bigger than that of corner subchannel. So the enthalpy difference between adjacent subchannels keeps the same sign along flow direction. The sign of turbulent mixing coefficient β is decided by the local enthalpy gradient at the subchannel interface.

In order to obtain detailed information of turbulent mixing factor, three axial positions, i.e. z=0.3 (positive β), z=0.9m (about zero β) and z=1.5m (negative β) are extracted to illustrate the development of local enthalpy gradient versus the flow direction. Draw a line to connect the center subchannel and side subchannel with the centroids. The local enthalpy gradient is plotted on the lines at different axial locations with such definition:

$$q_{mix} = \frac{\mu_t}{\Pr_t}\frac{\partial H}{\partial x} \tag{18}$$

Fig. 11 shows that the local enthalpy gradient at the center line between adjacent subchannels behaves like sinusoid. The zero point of q_{mix} is proximal to the interface line. At the location of z=0.3m, the zero point is at the left side of interface so q_{mix} <0 at the interface; At the location of z=0.9, the zero point is almost at the interface and q_{mix} is nearly equal to zero; At the location of z=1.5m, the zero point is at the right side of the interface, and q_{mix} >0. It can be inferred from the picture that the magnitude and sign of the turbulent mixing factor is related to the local enthalpy gradient at the interface. The alteration of the zero enthalpy gradients relative to the subchannel interface brings about the change of turbulent mixing factor.

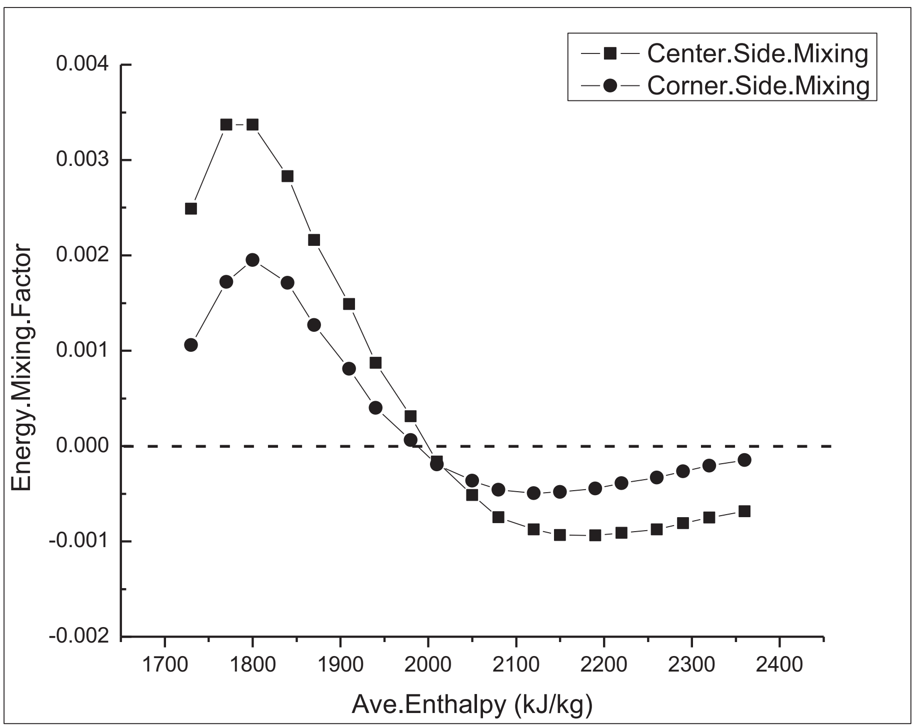

Fig. 9 The turbulent mixing coefficient calculated by energy mixing method

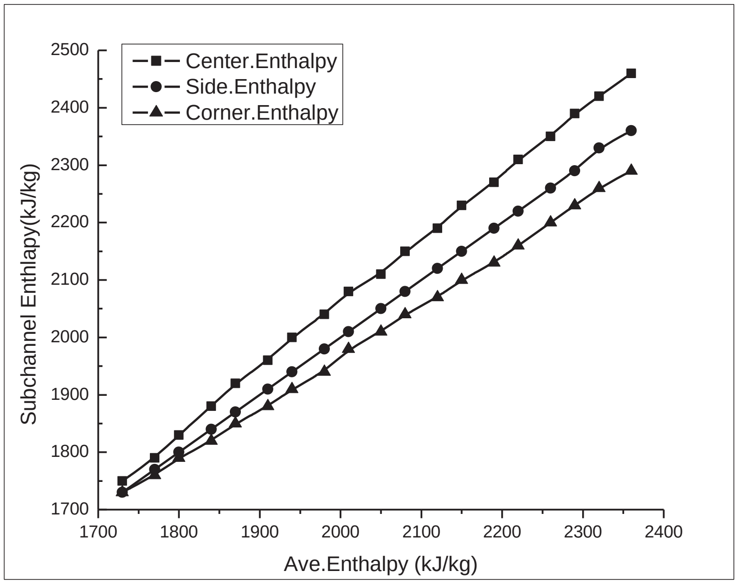

Fig. 10 The enthalpy increase for center, side and corner subchannels

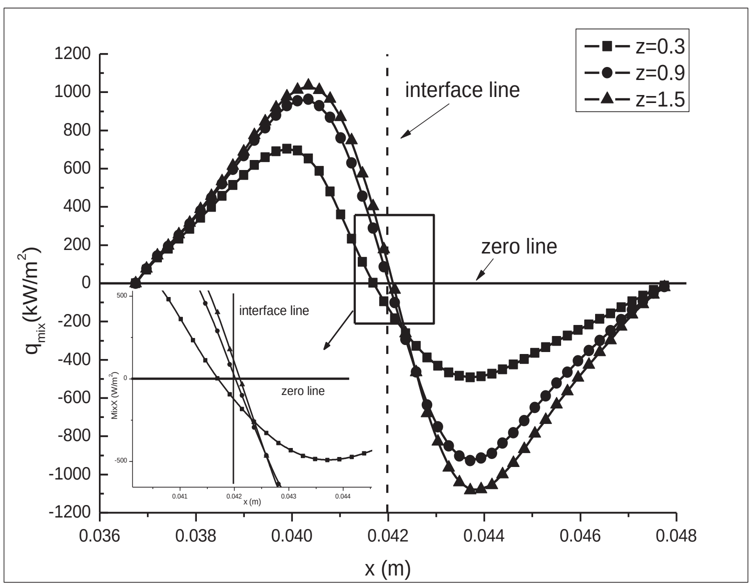

Fig. 11 The local enthalpy gradient at different locations

The zero point of local enthalpy gradient is at the neighborhood of the interface because the flow resistance is very obvious at this place leading to low mass flow rate and high fluid temperature. At the same time, its specific location is influenced by the secondary flow at the cross section. If we compare Fig. 9 and Fig. 7 together, a good correspondence will be found that the turbulent mixing factor is negative when the secondary flow is clockwise, while positive when the secondary flow is counterclockwise.

Such phenomenon can also be found in other kind of channels, shown in Fig. 12. The gap size between the wall and the fuel rod is enlarged from 1mm to 2mm thus increasing the hydraulic diameter of the side subchannel and the corner subchannel, decreasing the flow resistance. The secondary flow is always counterclockwise from the center subchannel to the corner and side subchannels. Fig. 12 presents the scheme picture of the secondary flow at the location of z=0.3m which makes an apparent comparison with the one with gap size equal to 1mm. Consequently, the turbulent mixing factor is always negative along the full way.

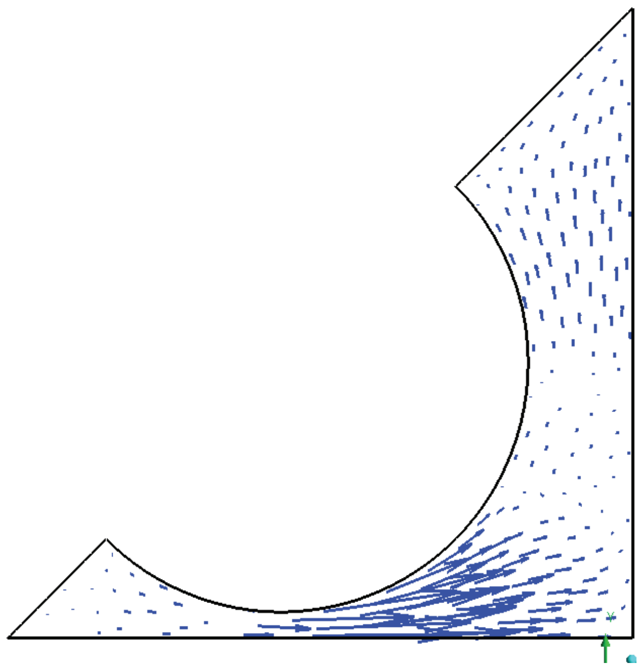

(a) Secondary flow at the cross section

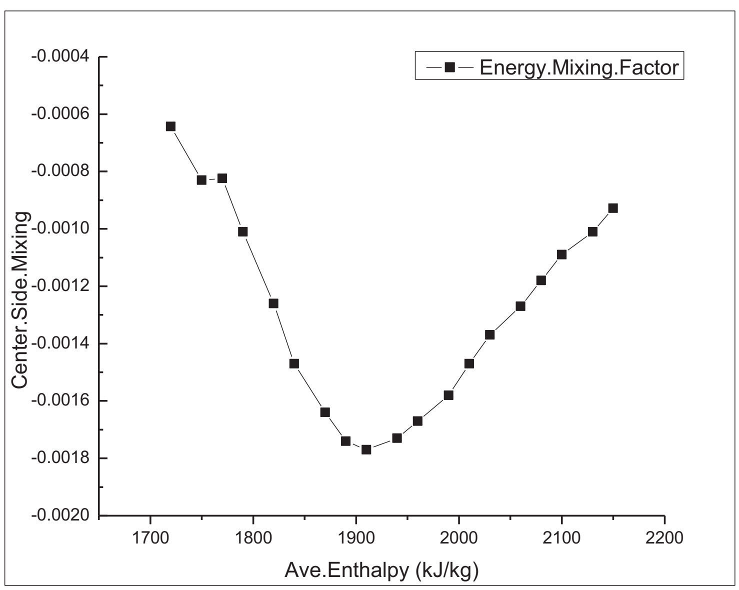

(b) turbulent mixing coefficient

Fig. 12 The corresponding relationship between the secondary flow direction and turbulent mixing coefficient after the gap is increased

3.3 Comparison with subcritical correlations

It is still hard to directly evaluate the turbulence mixing factor under supercritical conditions due to the lack of related experiments. Many researchers have devoted to the heat transfer coefficient and friction coefficient of supercritical water. Because of the big difference of fluid property between the boundary layer and the bulk fluid region, a correction factor accounting for such effect should be included. Whether the variation of fluid property will have effects on the turbulence mixing factor is still an open question. Here we just follow the same way of obtaining turbulent mixing factor as that under subchannel conditions and give a basic idea of the turbulent mixing factor.

Turbulent heat transport is related to subchannel enthalpy, eddy viscosity and $w_{ij}^{'}$

$$\beta\bar{G}\left(h_i - h_j\right) = \rho\varepsilon_{H_{ij}}\left[d\bar{h}/dz\right]_{ij} \tag{19}$$

Introducing a linear enthalpy gradient

$$\left[d\bar{h}/dz\right]_{ij} \approx \left(h_i - h_j\right)/z_{ij} \tag{20}$$

Here z_{ij} is the effective mixing distance between subchannels i and j; ε_{Hij} is the eddy diffusivity of heat transfer which is often related to eddy diffusivity of momentum according to Reynolds analogy:

$$\varepsilon_{H_{ij}} = \frac{\varepsilon_M}{\mathrm{Pr}_t} \tag{21}$$

The eddy diffusivity of momentum is different for supercritical water from that under subcritical conditions. The material property correction factor should be considered[J.G.Zang 2012].

$$\varepsilon_M = \kappa y u_\tau \left(\frac{\rho_w}{\rho}\right)^{1/2} = \kappa y^+ \left(\frac{\rho_w}{\rho}\right)^{1/2} v \tag{22}$$

According to definition of the friction velocity:

$$\tau_w = \rho_w u_\tau^2 = \frac{c_f}{2}\rho_b u_b^2, u_\tau = \sqrt{\frac{\rho_b}{\rho_w}}\sqrt{\frac{c_f}{2}}u_b \tag{23}$$

Define *s* as characteristic length.

$$\varepsilon_M = \kappa s\left(\frac{\rho_w}{\rho_b}\right)^{1/2}\sqrt{\frac{\rho_b}{\rho_w}}\sqrt{\frac{c_f}{2}}u_b = \kappa s\sqrt{\frac{c_f}{2}}u_b = \kappa s\sqrt{\frac{f}{8}}u_b \tag{24}$$

So we get the basic form of the turbulent mixing factor:

$$\beta_{ij} = \rho\varepsilon_{H_{ij}}/\bar{G}z_{ij} = \frac{\kappa}{\mathrm{Pr}_t}\frac{\rho u_b}{\bar{G}}\frac{s}{z_{ij}}\sqrt{\frac{f}{8}} \propto \sqrt{f} \tag{25}$$

It could be found from equation (25) that the turbulent mixing factor has the same form as that under subcritical conditions. Although the friction velocity and the eddy viscosity are both dependant on the density ratio, they finally balance out except the possibility that frictional coefficient could have material property correction factor itself. This could be a sign of the possibility of extrapolating subcritical formulas to supercritical conditions.

Some subcritical formulas of calculating the turbulent mixing factors are listed below (Jeong et al. 2007):

Rowe and Angle:

$$\beta = 0.0062\left(\frac{\overline{d_e}}{c}\right)\left(\frac{\overline{G}}{G_i}\right)\mathrm{Re}^{-0.1}, S/d = 0.036 \qquad (26)$$

$$\beta = 0.0021\mathrm{Re}^{-0.1}, \quad S/d = 0.149 \qquad (27)$$

Rogers and Rosehart (1):

$$\beta = 0.004\left(\frac{\overline{d_e}}{c}\right)\left(\frac{\overline{G}}{G_i}\right)\mathrm{Re}^{-0.1} \qquad (28)$$

Rogers and Rosehart (2):

$$\beta = 0.005\left(\frac{\overline{d_e}}{d}\right)\left(\frac{c}{d}\right)^{-0.894}\mathrm{Re}^{-0.1} \qquad (29)$$

Petrunik:

$$\beta = 0.009\left(\frac{d_e}{c}\right)\mathrm{Re}^{-0.173} \qquad (30)$$

Moyer:

$$\beta = \frac{\sqrt{2a}}{40}\frac{d_e}{\delta_{ij}}\mathrm{Re}^{-0.1}, \quad a = 0.046 \qquad (31)$$

Seal:

$$\beta = 0.02968\,\mathrm{Re}^{-0.1}, S/d = 0.1 \qquad (32)$$

$$\beta = 0.01683\,\mathrm{Re}^{-0.1}, S/d = 0.375 \qquad (33)$$

$$\beta = 0.009225\,\mathrm{Re}^{-0.1}, S/d = 0.833 \qquad (34)$$

Kelly and Todreas:

$$\beta = 0.007\,\mathrm{Re}^{-0.065}, S/d = 0.1, \quad 8000 < \mathrm{Re} < 24000 \qquad (35)$$

The physical meanings of the symbols appearing above are as follows:

Re-Average Reynolds number of adjacent subchannels

$\overline{d_e}$ -Average hydraulic diameter of adjacent subchannels

c -the gap size between adjacent subchannels

d -The diameter of the fuel rod

δ_{ij} The mixing length of adjacent subchannel

f_i The friction coefficient of subchannel i

Fig. 13 shows the comparison of turbulent mixing factors calculated by different formulas and the method based on the energy mixing of the CFD results. The Rowe & Angle and Seal formula give the prediction the magnitude of 9.0e-3, while Rogers & Rosehart(1), Rogers & Rosehart, Petrunik about 6e-3; Kelly and Todrea about 3e-3; Moye about 1e-3. These formulas are developed from experiments with a subchannel code by varying coefficients in an assumed mixing correlation and may be not sensitive to the local situation at the gap. The turbulent mixing factor calculated by CFD results has relatively big variation from the positive value at the entry to the negative at the outlet. The average of it along the flow channel is about 4.57e-4 which is smallest than other formulas considered here.

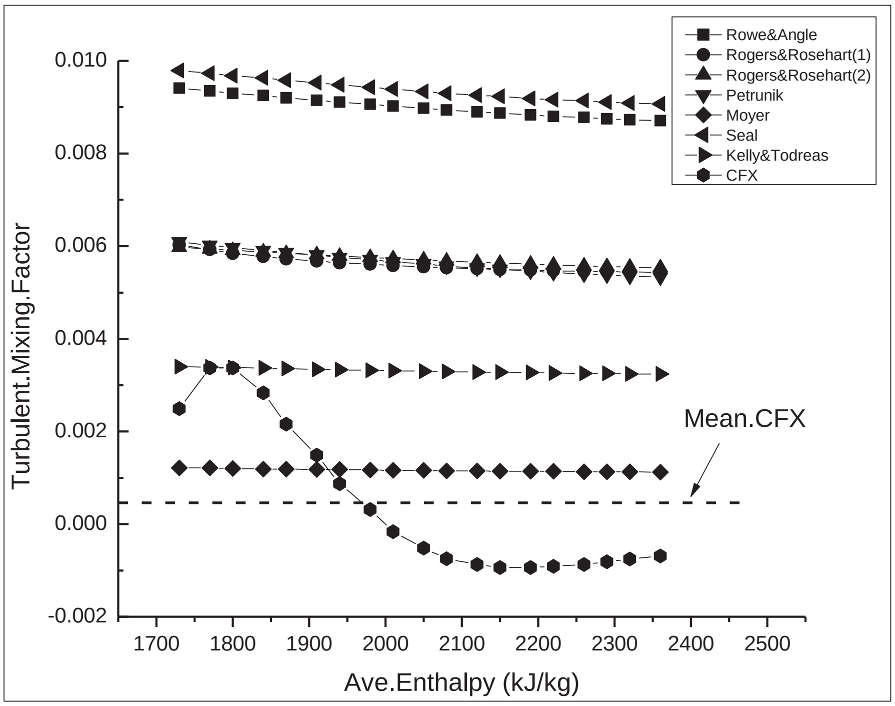

Fig. 13 Comparisons of various turbulent mixing formulas

In order to see whether such a small mixing coefficient is reasonable, the subchannel code ATHAS (Shan et al. 2009) was used to simulate the same case. ATHAS was developed by Xi'an Jiaotong University for fuel bundle analysis under supercritical conditions. The mixing coefficient could be specified at a fixed value by the user. Here the value of 4.57e-4 was used. Fig. 14 compares the variation of bulk fluid temperature of different subchannels predicted by ATHAS code and CFX software. The results are very close along the whole flow length which could provide a proof that such a small mixing coefficient is reasonable.

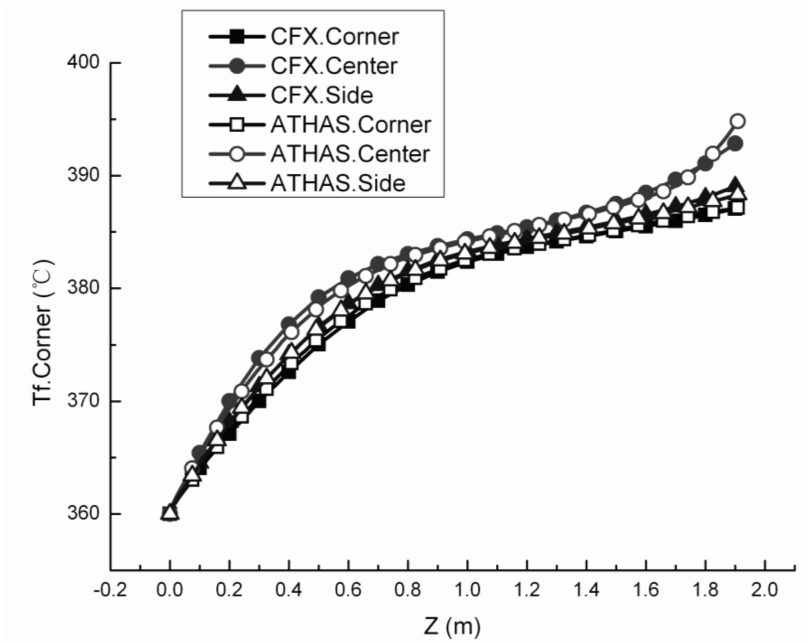

Fig. 14 The comparisons of subchannel analysis and CFD results

4. Conclusion

The turbulent mixing factor in 2×2 rod bundles at supercritical pressures is investigated through numerical analysis. The main conclusions obtained are as follows:

(1) The SST Model is selected as the turbulence model in this study due to its relatively better performance in dealing with heat transfer deterioration and complex geometry. The comparison with experimental data also supports this conclusion.

(2) For bare rod bundles, the main mechanism of heat exchange between two adjacent subchannels consists of diversion cross flow and turbulent mixing. Based on the energy conservation method, these two mechanisms are analyzed and compared. It has been found that the diversion cross flow has tight connections with the secondary flow pattern. Under supercritical conditions, both the geometry shape and the fluid property variation will influence the secondary flow.

(3) A new procedure of obtaining the turbulent mixing factor based on the energy mixing method is proposed in this study and compared with other two methods: the energy conservation method and the turbulent diffusion method. Both the energy mixing and energy conservation method predict the negative value of turbulent mixing factor which is very different from general opinions. The reason behind it is investigated and is believed to be related to the local enthalpy gradient.

(4) The possible expression form of the turbulent mixing factor is given following the similar way as that under subcritical conditions. The final form doesn't contain the fluid property factor explicitly except the friction coefficient which could be a sign of the possibility of extrapolating subcritical formulas to supercritical conditions. The comparisons of different turbulent mixing formulas show diverse effects ranging from 0.001 to 0.01. The average value of turbulent mixing factor calculated by energy mixing method was smallest compared with other formulas. The subchannel analysis with this value agrees well with the CFD results.

Nomenclature

A	Flow area(m^2)
c_f	Fanning frictional coefficient
c	The gap size between adjacent subchannel (m)
d	The diameter of the fuel rod (m)
$\overline{d_e}$	Average hydraulic diameter of adjacent subchannels (m)
f	Darcy-Weisbach frictional coefficient
G	Mass flux (kg m^{-2} s^{-1})
H or h	Fluid enthalpy(kJ/kg) or heat transfer coefficient (W m^{-2} K^{-1})
$h^{'}$	Fluctuation fluid enthalpy (kJ kg^{-1})
k	Turbulence kinetic energy (m^2 s^{-2})
$\Pr_t$	The turbulent Prandtl number
q_w	Wall heat flux (kW m^{-2})
Re	The Reynolds number
s	The characteristic length (m)
T_w , T_b	Wall temperature/ Bulk fluid temperature (K)
u	Fluid velocity (m s^{-1})
$u^{'}$, $v^{'}$	Fluctuation velocity component in flow direction and wall normal direction (m s^{-1})
u_τ	Friction velocity (m s^{-1})
U , V	Velocity component in flow direction and normal direction (m s^{-1})
V_{cross}	Cross flow velocity (m s^{-1})
y^+	Non-dimensional distance from the wall

Greek symbols

β	Turbulent mixing factor
δ_{ij}	The mixing length of adjacent subchannel (m)
ε	Rate of dissipation of k (m^2 s^{-3})
ε_M	Turbulent viscosity
ε_H	Turbulent viscosity of heat transfer (m^2 s^{-1})
κ	Von Karman constant
μ_t	Turbulent viscosity (m^2 s^{-1})
ρ	Fluid density (kg m^{-3})
τ	Wall shear stress (Pa)
ν	Momentum viscosity (m^2 s^{-1})
ω	Specific dissipation rate (s^{-1})

Subscript

b	Bulk
w	Wall
in	Inlet
out	Outlet
crossflow	Cross flow
Turb	Turbulence

Abbreviations

CFD	Computational Fluid Dynamics
SCWR	SuperCritical water Coold Reactor

References:

[1]. ANSYS. ANSYS Fluent theory guide.

[2]. B.V.Dyadyakin, A.S.Popov. 1977. Heat transfer and thermal resistance of tight seven-rod bundle coold with water flow at supercritical pressures. Transactions of VTI 11.244-53.

[3]. D. Palko, H. Anglart. 2008. Numerical study of heat transfer deterioration. Paper presented at the International Students Workshop on High Performance Light Water Reactors, Germany.

[4]. D.F. Torgerson, Basma A. Shalaby, Simon Pang. 2006. CANDU technology for Generation III+ and IV reactors. Nuclear Engineering and Design 236.1565-72.

[5]. Dae-Hyun Hwang , Yeon-Jong Yoo, Wang-Kee In,. 2000. Assessment of the interchannel mixing model with a subchannel analysis code for BWR and PWR conditions. Nuclear Engineering and Design 199.257-72.

[6]. G. Richards, A.S. Shelegov, P.L. Kirillov,et al. 2011. TEMPERATURE PROFILES OF A VERTICAL BARE 7-ELEMENT BUNDLE COOLED WITH SUPERCRITICAL FREON-12. Paper presented at the Proceedings of ICONE19, Chiba, Japan.

[7]. H.Y.Gu, X. Cheng, Y.H. Yang. 2008. CFD analysis of thermal-hydraulic behavior in SCWR typical flow channels. Nuclear Engineering and Design 238.3348-59.

[8]. —. 2010. CFD analysis of thermal-hydraulic behavior of supercriticalwater in sub-channels. Nuclear Engineering and Design 240.364-74.

[9]. Hae-Yong Jeong, Kwi-Seok Ha, Young-Min Kwon, et al. 2007. A dominant geometrical parameter affecting the turbulent mixing rate in rod bundles. International Journal of Heat and Mass Transfer 50.908-18.

[10]. J.G.Zang, X.Yan, S.F.Huang,et al. 2012. Analytical Prediction of Turbulent Friction Factor In Circular Pipe Under Supercritical Conditions. Paper presented at the ICONE20POWER2012, Anaheim, California.

[11]. J.Q.Shan , B. Zhang, C.Y. Li, et al. 2009. SCWR subchannel code ATHAS development and CANDU-SCWR analysis. Nuclear Engineering and Design 239.1979 – 87.

[12]. J.Yang, Y. Oka, et al. 2007. Numerical investigation of heat transfer in upward flows of supercritical water in circular tubes and tight fuel rod bundles. Nuclear Engineering and Design 237.420-30.

[13]. M. Sadatomi, A. Kawahara, K. Kano, et al. 2004. Single- and two-phase turbulent mixing rate between adjacent subchannels in a vertical 2 ×3 rod array channel. International Journal of Multiphase Flow 30.481-98.

[14]. Nicolás Silin, Luis Juanicó, Dar´ıo Delmastro. 2004. Thermal mixing between subchannels: measurement method and applications. Nuclear Engineering and Design 227.51–63.

[15]. Pioro, I. L., Duffey,R.B. 2007. Heat transfer and hydraulic resistance at supercritical pressures in power-engineering applications: ASME Press.

[16]. Q.L.Wen, H.Y.Gu. 2011. Numerical investigation of acceleration effect on heat transfer deterioration phenomenon in supercritical water. Progress in Nuclear Energy 53.480-86.

[17]. T. Misawa, T. Nakatsuka, H. Yoshida, K. Takase. 2009. Heat Transfer Experiments and Numerical Analysis of Supercritical Pressure Water in Seven-rod Test Bundle. Paper presented at the The 13th International Topical Meeting on Nuclear Reactor Thermal Hydraulics (NURETH-13) Kanazawa City, Ishikawa Prefecture, Japan.

[18]. T. Schulenberg, J. Starflinger, P. Marsault, et al. 2010. European supercritical water cooled reactor. Nuclear Engineering and Design 241.3505-13.

[19]. V.G. Razumovskiy, E.N. Pis'mennyy, A.E. Koloskov,et al. 2008. HEAT TRANSFER TO

SUPERCRITICAL WATER IN VERTICAL 7-ROD BUNDLE. Paper presented at the ICONE16, Orlando, Florida, USA.

[20]. V.G. Razumovskiy, Eu.N. Pis'mennyy, A.Eu. Koloskov, I.L. Pioro. 2009. HEAT TRANSFER TO SUPERCRITICAL WATER IN VERTICAL ANNULAR CHANNEL AND 3-ROD BUNDLE. Paper presented at the ICONE17, Brussels, Belgium.

[21]. Y. Zhu, E. Laurien. 2010. Numerical Investigation of Supercritical Water Cooling Channel Flows around a Single Rod with a Wrapped Wire. Paper presented at the Proceedings of ICAPP'10, San Diego, California, USA,.

[22]. Y.OKa, S.Koshizuka, Y.Ishiwatari, A. Yamaji. 2010. Super Light Water Reactors and Super Fast Reactors New York: Springer.

[23]. Z. Shang. 2009. CFD investigation of vertical rod bundles of supercritical water-cooled nuclear reactor. Nuclear Engineering and Design 239.2562-72.

[24]. Z.G.Huang, X.K.Zeng, Y.L.Li, et al. 2012. Numerical simulation of heat transfer deterioration in circular pipe of supercritical water. Nuclear Power Engineering (Chinese) 33.66-70.